

## A simultaneous and Sensitive Determination of Hydroquinone and Catechol at Anodically Pretreated Screen-Printed Carbon Electrodes

Sheng-Ming Wang, Wan-Yu Su, Shu-Hua Cheng\*

Department of Applied Chemistry, National Chi Nan University, Puli, Nantou Hsien, Taiwan 545

\*E-mail: [shcheng@ncnu.edu.tw](mailto:shcheng@ncnu.edu.tw)

Received: 18 August 2010 / Accepted: 15 September 2010 / Published: 1 November 2010

---

Hydroquinone (HQ) and catechol (CA) are two positional isomers of dihydroxybenzene. They usually coexist in environmental samples and bring about pollution in our living environment. This research has developed a cheap, sensitive, and rapid method for the electrochemical determination of HQ and CA in aqueous pH 6.0 buffer solution without previous separation. By employing both anodically pretreated screen-printed carbon electrodes (SPCE\*) and square wave voltammetric techniques, a direct and simultaneous determination of the two positional isomers was achieved. The oxidation peak potentials for HQ and CA were completely separated at the SPCE\*, exhibiting well-defined and quasi-reversible redox peaks and showing greatly enhanced activity. Under optimized conditions, the linear calibration ranges for HQ and CA were in the ranges of 0.1-50 and 0.1-70  $\mu\text{M}$ , with detection limits ( $S/N = 3$ ) of 0.05 and 0.05  $\mu\text{M}$ , respectively. This method was applied to the direct determination of HQ and CA in river water with satisfactory recovery results.

---

**Keywords:** Hydroquinone, Catechol, anodization pretreatment, screen-printed carbon electrode, square wave voltammetry.

### 1. INTRODUCTION

Hydroquinone (HQ) and catechol (CA) are two positional isomers of dihydroxybenzene. They have been extensively studied due to their biological and environmental importance. HQ and CA can coexist in an aquatic environment as a result of their widespread use in pesticides, wood preservatives, tanning lotion, cosmetic creams, dyes and synthetic intermediates. Phenol and its derivatives found in the waste effluents of industrial processes and agricultural activities are common organic pollutants with high toxicities. They thus represent a serious environmental threat [1]. Pyrolysis from tobacco

smoke also produces phenolic derivatives causing air pollution [2]. Therefore, it is a demanding subject to establish a fast, selective and sensitive detection method for phenol pollutants in environmental samples.

Previous separation and chemometric treatments are often introduced prior to isomer analysis. Direct quantitative determination of dihydroxybenzene isomers using traditional spectrophotometry suffers interference difficulties due to the similar structures and properties of isomers [3]. While high-performance liquid chromatography is a good option for the determination of isomers [1], the procedures are time-consuming.

Other methods such as synchronous fluorescence [2], biosensing [4], and capillary electrochromatography [5], have been developed to determine the isomers.

Electrochemical methods have been proposed as efficient alternatives due to their low cost, rapid analysis, high sensitivity and good selectivity [6-12]. Both HQ and CA have electroactive quinone structures and possess similar electrochemical activity. Therefore, electroanalyses are employed for the determination of a single analyte, either HQ [8] or CA [7,12]. In a binary mixture containing both HQ and CA, a considerable overlap oxidation signal was observed [6,10]. An application of neural networks with pruning can solve the problem by modeling overlapping peaks [6]. In addition, derivative techniques have been used to separately determine organic isomers [13].

The simultaneous determination of organic isomers through the use of conventional electrodes is a more challenging subject. In recent years, a few reports have focused on the preparation of functionalized electrodes and an exploration the voltammetric determination of isomers. For example, a simultaneous determination for naphthol isomers was achieved on glassy carbon electrodes (GCE) modified with electropolymerized acridine orange film [14] and carbon nanotubes-Pt nanoparticles [13]. Wang fabricated modified electrodes with nanometer-sized composite films for a simultaneous detection of aminophenol isomers [15].

The simultaneous determination of dihydroxybenzene isomers has been investigated on chemically modified electrodes with conductive organic polymers and nanomaterials as modifiers [16-25]. The research results are listed in Table 1. However, these methods still suffer from the tedious preparation (modification) processes. It is therefore important to develop a simple, fast, highly sensitive and selective electrochemical method for the simultaneous determination of dihydroxybenzene isomers.

Various surface pretreatment methods have been reported to improve the electrochemical performance of carbon electrode surfaces. Among these procedures, electrochemical pretreatment is used extensively due to its conveniences.

The electrochemical activity of carbon materials, such as GCE and SPCE (screen-printed carbon electrodes), can be significantly enhanced by electrochemical anodization or potential cycling [26-37]. Reports suggest that the carbon surface re-orientates to generate more edge-plane sites and introduces oxygen-containing functionalities at the carbon surface subsequent to the electrochemical pretreatment, acting more or less like edge-plane graphites or carbon nanotubes.

The pretreated carbons have shown greatly improved electroactivity and present a promising application for the determination of lead ion [26,27], nitrotyrene [28] and biomolecules [29-35].

**Table 1.** Summary of electroanalytical results for the simultaneous detection of HQ and CA.

electrode	method	solution	analytes	linear range ( $\mu\text{M}$ )	DL ( $\mu\text{M}$ )	Ref.
GCE/SWCNT	2.5 <sup>th</sup> -order DV <sup>a</sup>	pH 5.6	HQ	0.4-10	0.12	16
			CA	0.4-10	0.26	
GCE/SWCNT/polymer <sup>b</sup>	first-order DV <sup>a</sup>	pH 6.5	HQ	1-100	0.1	17
			CA	1-100	0.1	
GCE/MWCNT	first-order DV <sup>a</sup>	pH 5.5	HQ	2-100	0.6	18
			CA	2-100	0.6	
Pt/mesoporous Pt film	DPV <sup>g</sup>	pH 1.0	HQ	50-2000	-----	19
			CA	20-1000	-----	
GCE/ Nafion-CMK-3 <sup>c</sup>	CV	pH 7	HQ	1-30	0.7	20
GCE/MWCNT	DPV <sup>g</sup>	pH 4.5	HQ	1-100	0.75	21
			CA	0.6-100	0.2	
GCE/polymer <sup>d</sup>	DPV <sup>g</sup>	pH 5	HQ	5-80	1	22
			CA	1-60	0.5	
GCE/polymer <sup>e</sup>	DPV <sup>g</sup>	pH 5	HQ	10-140	1	23
			CA	10-140	0.7	
GCE/polymer <sup>f</sup>	DPV <sup>g</sup>	pH 4.5	HQ	5-80	1	24
			CA	1-80	0.8	
GCE/MWCNT Multi-electrode array	amperometry	pH 5.4	HQ	1-100	0.3	25
			CA	1-100	0.2	
SPCE*	SWV	pH 6	HQ	0.1-50	0.05	this work
			CA	0.1-70	0.05	

- a. derivative voltammetry
- b. poly(acid chrome blue K)
- c. a mesoporous carbon material
- d. poly(glycine)
- e. poly(phenylalanine)
- f. poly(glutamic acid)
- g. differential pulse voltammetry

In this study, the SPCE was pretreated at a high anodization potential and used to simultaneously sense HQ and CA. The SPCE\* exhibited high electrocatalysis and recognition abilities regarding the two isomers. Two well-defined oxidation peaks, along with high current responses, were achieved using square wave voltammetry. The proposed method has been applied to simultaneous determinations of HQ and CA in real samples with satisfactory recoveries.

## 2. EXPERIMENTAL

### 2.1. Reagents

Hydroquinone and catechol were obtained from Acros (USA). These chemicals were of the highest available grade and used without further purification. All other chemicals were of analytical reagent grade and also obtained from Acros. All solutions were prepared using deionized water from a Milli-Q ultrapure water system with a resistivity of 18 M $\Omega$ cm. The various pH buffer solutions (0.1 M) were prepared as follows: citrate buffer solutions, pH 2.0-6.0; phosphate buffer solutions (PBS), pH 7.0-8.0, 12.0; borate buffer solutions, pH 9.0-10.0; carbonate buffer solutions, pH 11.0.

### 2.2. Instruments

Cyclic voltammetry was performed with a voltammetric analyzer (CHI, model 621C). A bare SPCE (geometric area 0.2 cm<sup>2</sup>) from Zensor R&D (Taiwan) was rinsed in deionized water before use and employed as the working electrode. A platinum wire was used as the counter electrode. A home-made Ag|AgCl|KCl (sat.) electrode was used as the reference electrode. All potentials were reported with respect to this reference electrode. The experiments were carried out at room temperature (25 $\pm$ 2  $^{\circ}$ C) at bare (untreated) SPCE and electrochemical preanodized SPCE\*. Each electrode was used in a single assay. A Hitachi S-4700I high-resolution scanning electron microscopy (SEM) was used to characterize the electrode surface. Room temperature Raman spectra were recorded with a Ramboos 500i (DongWoo Optron, Korea) coupled a 3D nanometer scale Raman PL microscopy system. A semiconductor diode laser with a wavelength of 532 nm was employed. A CCD detector (Andor DU420A-BR-DD) cooled at -50  $^{\circ}$ C was used to record the Raman scattered light intensity. The pH of each buffer solution was measured with a Thermo Scientific Orion pH meter (model 420).

### 2.3. Analytical procedures

Electrochemical pretreatment was performed by anodizing the SPCE at 2.0 V for 900 s in PBS (pH 7.0) in order to obtain the activated SPCE\*. The preconcentration by adsorption (accumulation) of the analytes at the working electrode was carried out in a stirred solution at -0.3V for 180 s. The voltage-scanning step was initiated after 5 s of equilibrium time. Voltammetric measurements were performed in an aqueous 0.1 M phosphate buffer (pH 6.0) with varying concentrations of HQ and CA deaerated with pure nitrogen prior to, and during, the scan. The square wave voltammograms were recorded with parameters as follows: scan range, -0.2 to 0.5 V; amplitude, 50 mV; potential increment, 4 mV; frequency, 2 Hz.

## 3. RESULTS AND DISCUSSIONS

### 3.1. Cyclic voltammetric studies and adsorption features of HQ and CA

Fig. 1 depicts the cyclic voltammograms of the 10  $\mu$ M single-component solution of HQ and CA in pH 7.0 PBS at a scan rate of 0.1 V/s after conditioning at -0.3 V for 180 s. At bare SPCE, each

analyte showed broad, weak and ill-defined oxidation and reduction waves (Fig. 1A). However, the cyclic voltammograms changed dramatically, exhibiting an obvious increase in background and peak currents (Fig. 1B). The increased background current suggests the alteration of electrode surface after electrochemical pretreatment. Meanwhile, both the oxidation and reduction peak potentials were greatly lowered. The increase in the oxidation peak currents and the lowering of oxidation peak potentials are clear evidence of the catalytic effect of SPCE\* toward HQ and CA oxidation. This is in agreement with previous studies showing that increased electrochemical activity can be achieved at electrochemically pretreated electrodes for a wide range of reversible and irreversible redox processes [26-37]. At SPCE\*, the peak-to-peak potential separation ( $\Delta E_p$ ) equaled 0.080 and 0.084 V for HQ and CA, respectively. The calculated cathodic current to anodic current ratio ( $i_{pc}/i_{pa}$ ) was 0.93 and 0.92 for HQ and CA, respectively. The electrochemical characteristics suggest that the oxidations were quasi-reversible with half-wave potential ( $E_{1/2}$ ) located at 0.086 and 0.178 V for HQ and CA, respectively. These responses can be attributed to the oxidation of dihydroxybenzene to produce quinone and vice versa. With the increasing scan rate, the oxidation peak currents increase linearly with the scan rate (0.005-0.15 V/s), indicating that the electrode reaction was a typical adsorption-controlled process [13].

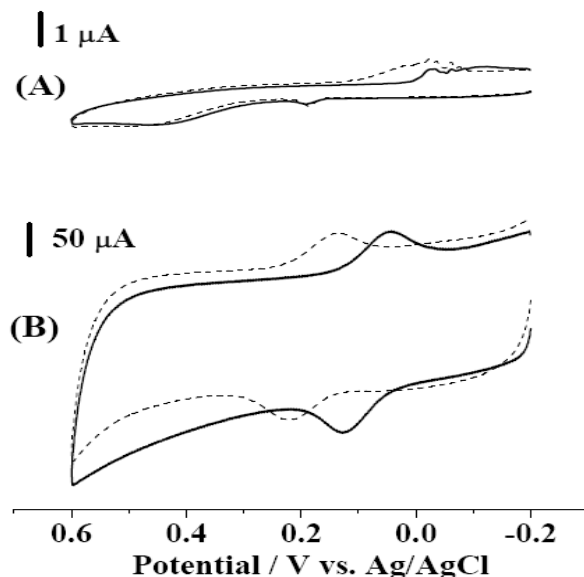


**Figure 1.** Cyclic voltammograms of (a) bare SPCE, and (b) SPCE\* in 0.1 M pH 7.0 buffer solution containing 10  $\mu\text{M}$  HQ (solid line) and CA (dash line) after preconcentration at -0.3 V for 180 s. Scan rate = 0.1 V/s.

The improved electroactivity at SPCE\* likely reflects a larger surface area, hence,  $\text{Fe}(\text{CN})_6^{3-}$  was selected as a probe. The slopes of peak current vs. scan rate<sup>1/2</sup> were 52.4 and 128.3  $\mu\text{A V}^{-1/2} \text{s}^{1/2}$  at SPCE and SPCE\*, respectively. The results suggest that the surface area of SPCE\* was 2.45 times that of SPCE; this draws from the electrochemical pretreatment, and leads to a more favorable exposure of

graphite particles and a higher electrochemically effective surface area. The SEM images reveal that surface morphology altered significantly from dense, aggregated nanosphere particles (Fig. 2A) to a rougher configuration of large pores, multi-layers and a sponge-like network honeycombed by nano-size cavities (Fig. 2B) after the preanodization processes.

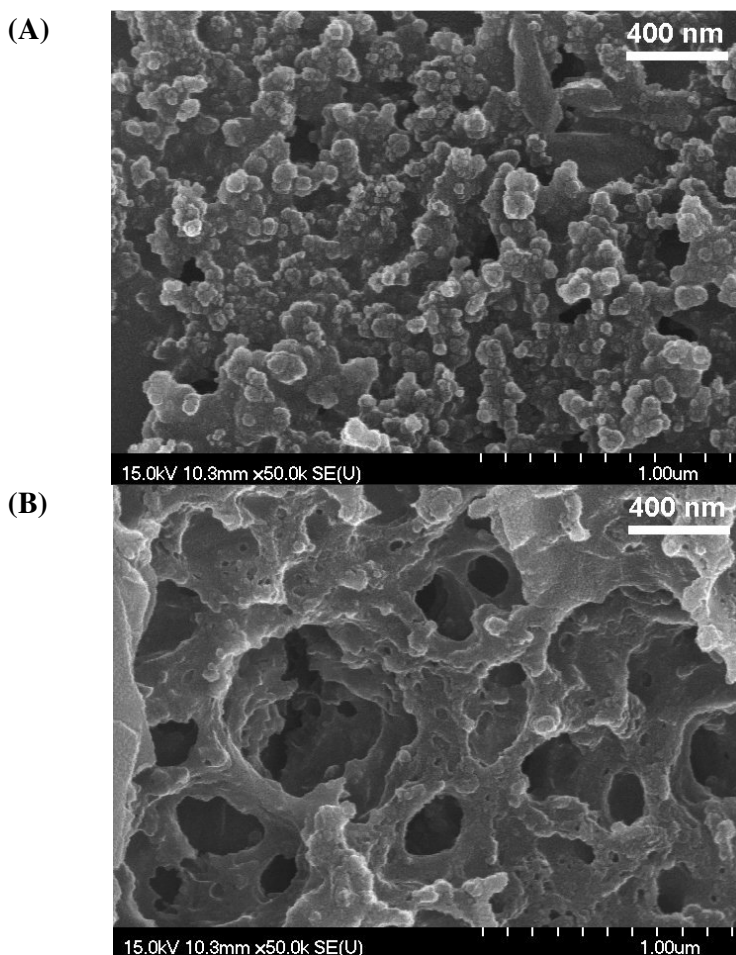


**Figure 2.** Scanning electron micrographs of (A) SPCE and (B) SPCE\*

Preanodization processes create a more porous and rougher surface; this larger surface area can promote a high proclivity for adsorption of HQ and CA on the SPCE\* surface. As shown in Fig. 3, the dotted line represent the background voltammetric response of SPCE\* in pH 7.0 buffer solutions without analytes. The solid line shows the cyclic voltammograms of SPCE\* in the same blank medium after immersing it in 10  $\mu$ M HQ (or CA) solutions and conditioning at -0.3 V for 180 s. A stable reversible redox couple appeared for HQ (Fig. 3A) and CA (Fig. 3B). The adsorption features are similar to those of previous reports in which phenolic compounds are easy to be adsorbed onto electrochemically activated carbon electrodes [38] and electrodes modified with multiwalled carbon

nanotube [21,39], mesoporous carbon materials [20] and mesoporous platinum [19]. On the other hand, an insignificant amount of adsorbed HQ and CA on the untreated SPCE was observed. Moreover, no redox wave appeared when immersing SPCE\* into a stirred 10  $\mu\text{M}$  HQ (or CA) solution for 60 min at open circuit potential and then transferring it to the blank buffer solutions, which implies an electrochemical adsorption effect [39].

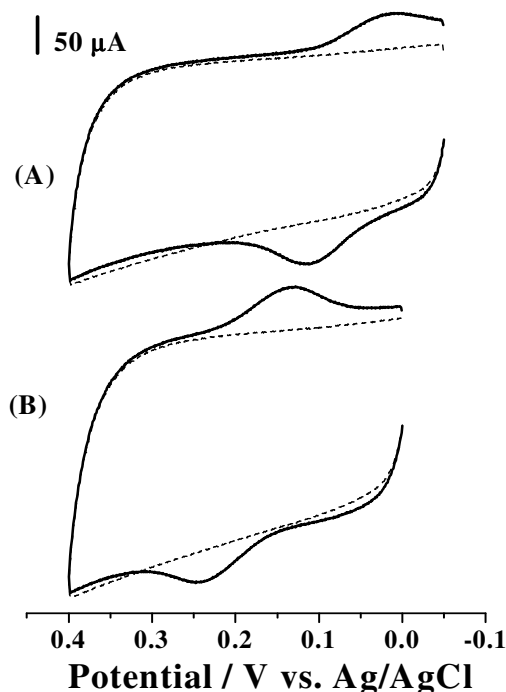


**Figure 3.** Cyclic voltammograms of the SPCE\* in 0.1 M pH 7.0 buffer solution before (dash line) and after (solid line) pre-concentration at -0.3 V for 180 s in 10  $\mu\text{M}$  (A) HQ (B) CA.

The peak current in Fig. 3 did not obviously decrease after 10 continuous cycles suggesting that HQ and CA were readily and strongly adsorbed onto the preanodized SPCE\*. With the aid of equation  $\Gamma = Q/nFA$ , the adsorption surface concentration ( $\Gamma$ ) was calculated from the value of the charge  $Q$  (the oxidation peak area of HQ and CA) and the electron transfer number  $n$  (here  $n$  was taken as 2). The calculated adsorption amounts of HQ and CA at SPCE\* were  $1.78 \times 10^{-9}$  and  $1.54 \times 10^{-9}$  mol/cm<sup>2</sup>, respectively. This suggests that HQ is apt to a greater adsorption on SPCE\* than CA is. A recent report also showed selective immobilization of CA on electrochemically activated carbon electrode, but dopamine (3,4-dihydroxyphenethylamine, DA) failed to show adsorption effect [38]. Our studies showed somewhat different results; both CA and HQ strongly adsorbed on SPCE\* without noticeable decrease in electroactivity. Dopamine also adsorbed on SPCE\* but suffered from decreased redox couple  $\Gamma_{\text{DA}}$  (data not shown). The differences may result from a longer time employed in the

anodization pretreatment during the electrode preparations. The above results indicate that preanodization processes result in increases in electrode surface area and porosity that leads to adsorption of HQ and CA.

Another factor that control the adsorption behavior is believed to be an increased number of edge-plane-like defects [29-35]. Fig. 4 shows the Raman spectrum of a bare SPCE before and after preanodization. Two weak bands, D at  $1358\text{ cm}^{-1}$  and  $E_{2g}$  at  $1594\text{ cm}^{-1}$ , were observed for bare SPCE. Upon preanodization at 2.0 V for 900 s, the intensity of both peaks increased and higher D/ $E_{2g}$  ratio was obtained. These observations indicate the introduction of more edge plane sites after the preanodization procedure [32]. Compton's research proposed that the edge-plane defects of carbon materials are active sites, responsible for the high electrocatalytic activity toward several biomolecules [40-42].

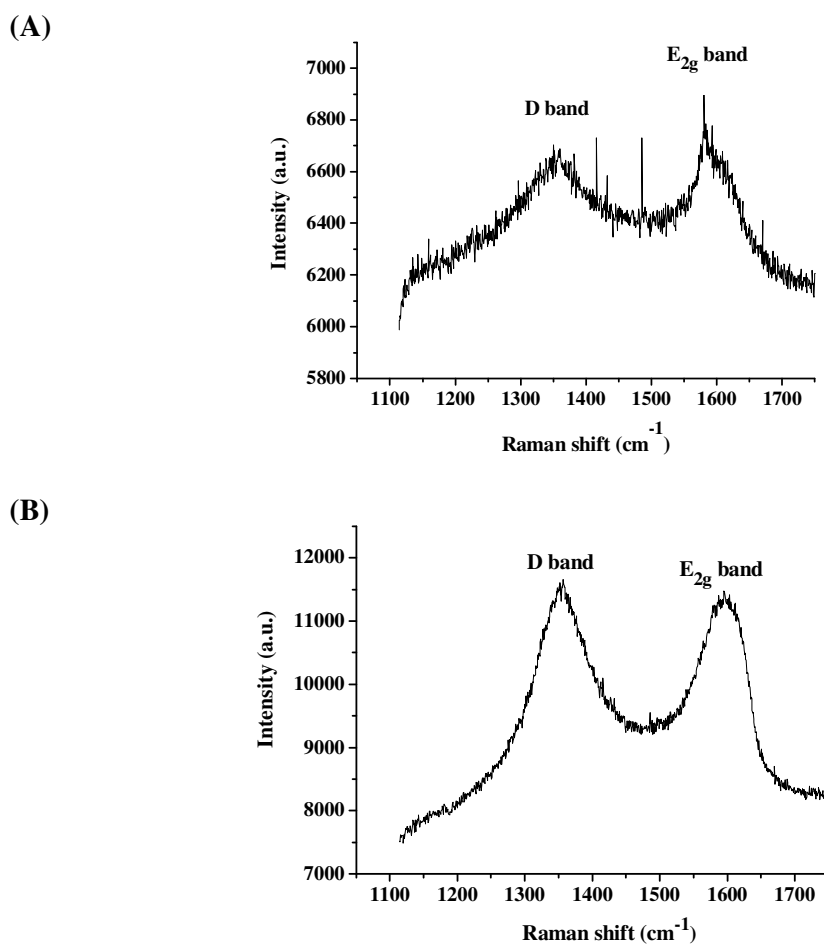


**Figure 4.** Raman spectrum of bare SPCE (A) before and (B) after preanodization at 2.0 V for 900 s. Laser power at sample was 90 mW at 532 nm with 5 s detector exposure.

The chemical transformation of carbon characteristics is also assumed to contribute the adsorption effects. The original SPCE surfaces are generally hydrophobic in character.



Electrochemical oxidation may result in the oxygen-covered SPCE\* surface and constitutes the polar sites [36] where HQ and CA are expected to be readily adsorbed, as a result of hydrophilic attraction or hydrogen bonding [39]. Although the interaction between electrode surface and analyte is not proved in this work, it is believed that the functional groups (-OH and -COOH) [26-37] and their distribution over the SPCE\* surface control the molecular recognitions of HQ and CA. As a consequence of the physical and chemical alterations in electrode surface, the electron transfer of HQ and CA at the SPCE\* occurred at different redox potentials with facilitated rates.

Owing to the strong adsorption of HQ and CA on SPCE\*, they do not easily leave the electrode surface, which is unfavorable to the reusability of electrodes. Although the electrode was passivated due to its adsorption characteristics, the problems were solved by the low cost, single-use, and disposable nature of the SPCE. Therefore, electrode refreshment is not necessary. Each electrode was used only once before disposal.

### *3.2. Optimization of experimental parameters*

From the above studies, the oxidation peak potential differences between HQ and CA can reach up to 100 mV. Thus, the oxidation peaks of both analytes could be separated and identified entirely at SPCE\*. In order to optimize the electrode activity, the electrode phase conditions and solution acidity were systematically investigated; these included: the electrochemical preanodization parameters, the preconcentration conditions and solution pH values.

The measurement to determine the optimum operational conditions was carried out in the presence of 10  $\mu$ M CA.

### *3.3. Studies on the preanodization parameters*

It was observed that both preanodization potentials and electrolysis time have a great impact on electrode responses. The preanodization potential dependence of the CA response at the SPCE\* was examined and the results are shown in Fig. 5A. By keeping the preanodization time as 900 s, the current responses over the preanodization potential range of 0.5 to 2.3 V were studied in 0.1 M PBS (pH 7.0) containing 10  $\mu$ M CA. No obvious anodic peak currents were observed when the preanodization potentials were less than 1.5 V.

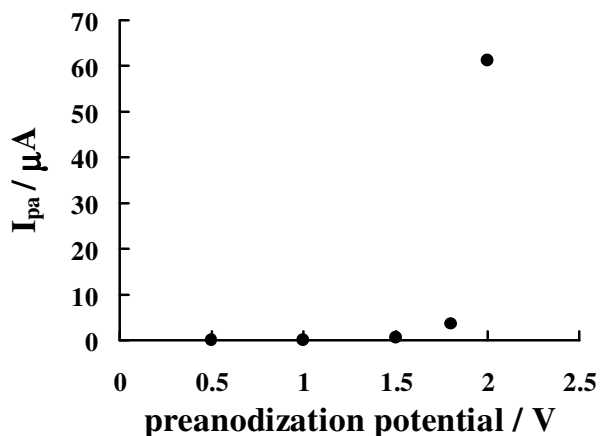
A sharply enhanced oxidation current was observed at 2.0 V. More extreme potentials displayed poor reproducibility in current responses. The effect of preanodization time (at 2.0 V) on the current response was recorded, and is shown in Fig. 5B.

A smooth increase in the peak current was observed upon extending the preanodization time from 60 to 900 s; it reached a maximum at 900 s. A decrease in the response was observed when beyond 900 s. The results suggest that the excessively high preanodization potential and time do not necessarily imply the high performances in electrochemical detection. This suggests that the redox activity of SPCE\* toward CA oxidation is highly dependent upon the preanodization processes.

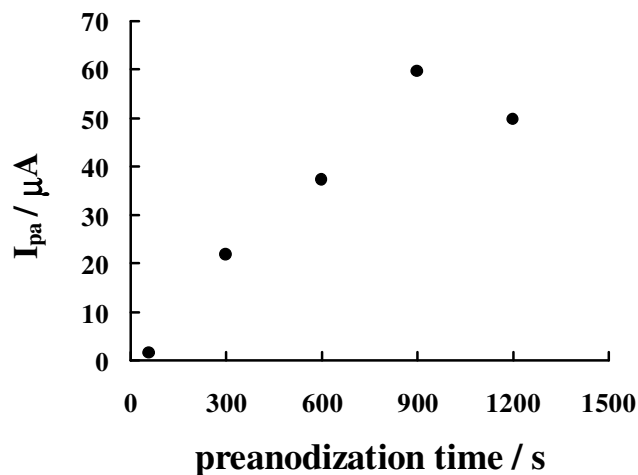
### 3.4. Studies on the preconcentration conditions

The preconcentration step is a major process for adsorbing analytes onto electrode surfaces. The adsorbate molecules should first be transported from the bulk solution to the electrode surface and become immobilized. There will be no mass transfer effect if the solution is well stirred. The adsorption quantity is thus controlled primarily by the properties of the adsorbate molecules and the surface state of the electrode. Preconcentration conditions were investigated through a process of constant stirring of 10  $\mu\text{M}$  CA in pH 7.0 PBS. Fig. 5C shows the effects of preconcentration time on the magnitude of the current signal as a result of adsorption of SPCE\*. Under open-circuit potential conditions, no oxidation currents were observed when the accumulation time changed from 60 to 300 s. At applied potentials of 0.0,  $-0.2$  and  $-0.3$  V, the oxidation currents increased with time; it reached a maximum at 180 s and then became a plateau when beyond 180 s. Therefore, 180 s accumulation time at  $-0.3$  V was used throughout the experiments.

(A)



(B)



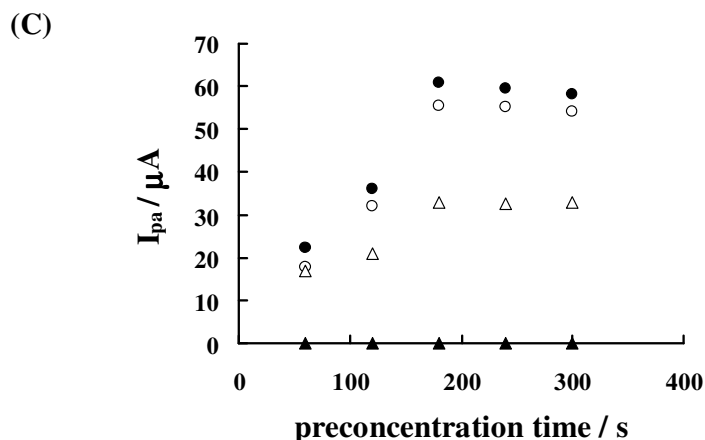


**Figure 5.** Plot of oxidation peak current versus (A) preanodization potential (B) preanodization time (C) pre-concentration time at open circuit ( $\blacktriangle$ ), 0 V ( $\triangle$ ), -0.2 V ( $\circ$ ) and ( $\bullet$ ) -0.3 V. The solution was 10  $\mu M$  of CA in pH 7.0 phosphate buffer solution.

### 3.5. pH effects

The electro-oxidation of HQ and CA is considered a proton-participating reaction so the solution acidity will affect the electrode reaction process. Cyclic voltammograms revealed that both the cathodic and anodic peak potentials of HQ and CA negatively shifted with the increase of pH from 4.0 to 8.0. The oxidation peak potential varies linearly with slopes of  $-64.3$  and  $-64.1$  mV/pH for HQ and CA, respectively (Fig. 6A). The results are in agreement with the potential shift predicted by the Nernst equation, suggesting that the oxidation involves 2-electron and 2-proton reactions [21]. Fig. 6B illustrates the variation in oxidation peak currents of HQ and CA on changing solution pH values. It can be seen that the oxidation peak currents of HQ and CA slightly increase as the pH is increased from 4.0 to 6.0. The peak currents decrease as the pH is increased from 6.0 to 8.0, presumably due to instability in the weak alkaline media. Electrostatic repulsion between the analytes and the electrode might also contribute to the reduced peak current [21]. The functional groups  $-\text{COOH}$  at the SPCE\* may become deprotonated and possess negative charges in pH 8.0 medium, where partial HQ and CA can become deprotonated as anions. In order to obtain a high sensitivity, a pH 6.0 buffer solution was chosen for the following analytical assays. Drawing from the above experimental studies, the optimized parameters for high current responses and good reproducibility were as follows: preanodization potential, 2.0 V; preanodization time, 900 s; pre-concentration potential, -0.3 V; pre-concentration time, 180 s; and solution pH, 6.0.

### 3.6. Analytical application.

Square wave voltammetry (SWV) has been used to improve analytical performance due to its high sensitivity [31]. Fig. 7 shows the SWV at SPCE\* for a mixture of two analytes under optimized

conditions. Two absolutely separated peaks were visualized and the calibration graphs were obtained. The oxidation peak currents increased linearly with increasing concentrations ranging from 0.1 to 50  $\mu\text{M}$  for HQ. The regression equation was  $I (\mu\text{A}) = 14.56 \times C (\mu\text{M})$ ,  $R^2 = 0.9901$ . The detection limit ( $S/N = 3$ ) for HQ was estimated to be 0.05  $\mu\text{M}$ . The oxidation peak current vs. CA concentration was linear in the range of 0.1 to 70  $\mu\text{M}$ .

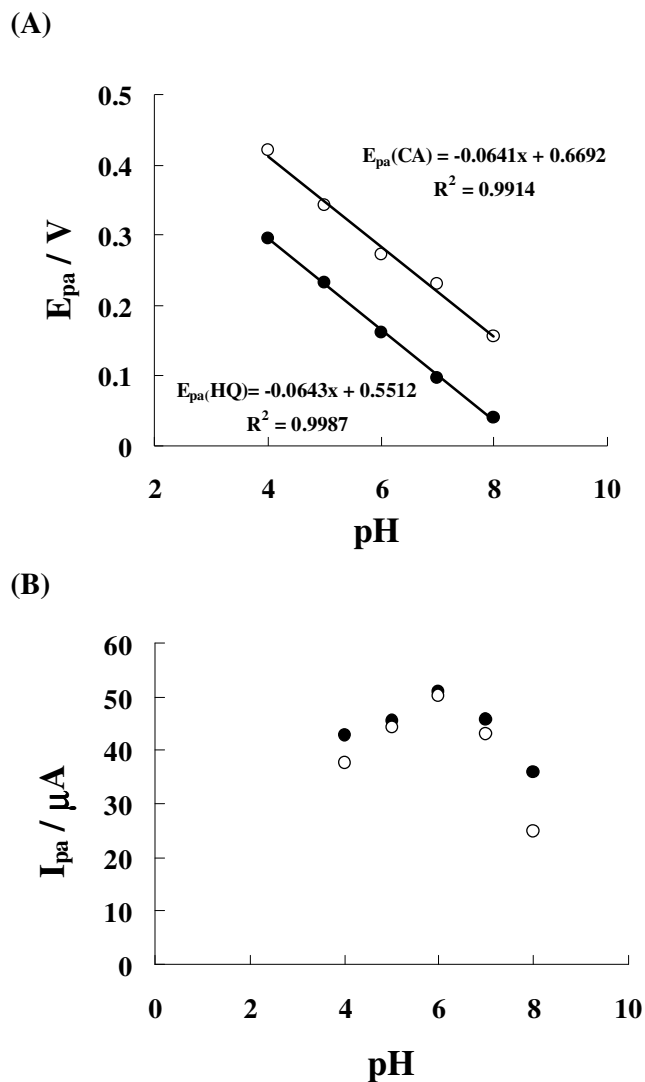


**Figure 6.** Plot of (A) peak potential (B) peak current versus pH for HQ (●) and CA (○).

The regression equation was  $I (\mu\text{A}) = 11.19 \times C (\mu\text{M})$ ,  $R^2 = 0.9908$ . The detection limit ( $S/N = 3$ ) for CA was estimated to be 0.05  $\mu\text{M}$ . The higher sensitivity for HQ over CA suggests that the response differences were associated with the shape-selective property of the activated carbon surfaces. The relative standard deviations (RSD) for 50  $\mu\text{M}$  HQ and CA standards were 1.82% and

1.47%, respectively, for three independent SPCE\*, revealing no significant differences between prepared electrodes.

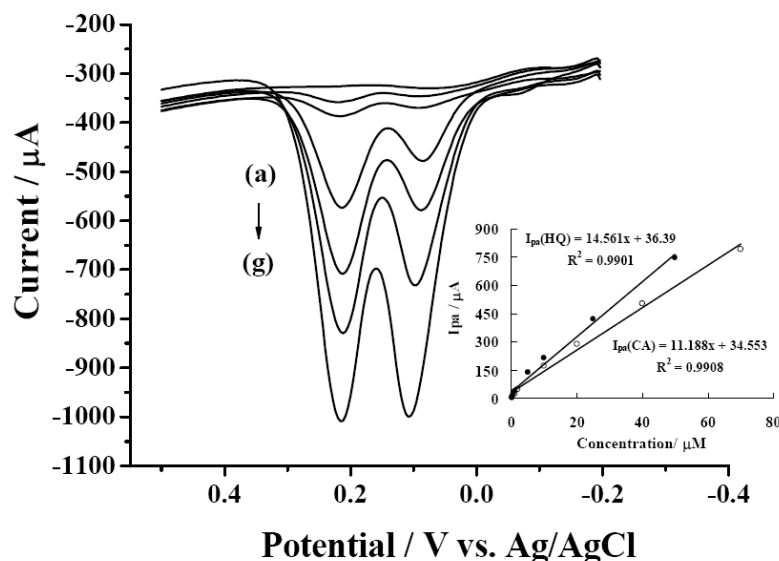


**Figure 7.** Square wave voltammograms at SPCE\* in pH 6.0 buffer solution containing various concentration of HQ+CA ( $\mu\text{M}$ ). (a) 0.1+0.1 (b) 0.5+1.0 (c) 1.0+2.0 (d) 5.0+10.0 (e) 10.0+20.0 (f) 25.0+45.0 (g) 50.0+70.0. The inset shows the plot of  $I_{pa}$  vs. concentration.

**Table 2.** Results of the recovery tests for hydroquinone and catechol using the proposed square wave voltammetric method.

Matrix	Spiked ( $\mu\text{M}$ )		Found ( $\mu\text{M}$ )		Recovery (%)	
	hydroquinone	catechol	hydroquinone	catechol	hydroquinone	catechol
river water <sup>a</sup>	0	0	-----	-----	-----	-----
	1	2	0.986	2.067	98.6	103.3
	5	10	5.038	10.608	100.7	106.1
	10	20	10.678	22.746	106.8	101.8
	25	40	26.680	43.343	106.7	108.4

a. obtained from Nangang River in Puli, Taiwan.

The selective determination of various HQ concentrations in the presence of a constant CA concentration using SWV was also investigated at SPCE\* and vice versa. Fig. 8A shows the SWV recorded for 0.5-50  $\mu\text{M}$  of HQ in the presence of 5.0  $\mu\text{M}$  of CA. Clearly, there was a monotonical increase in peak current corresponding to the oxidation of HQ with the increase in HQ concentration,

while the oxidation peak current of CA stayed almost constant. SWVs recorded for 1.0-70  $\mu\text{M}$  CA at a constant HQ concentration of 5.0  $\mu\text{M}$  are presented in Fig. 8B. Again, the data show that there is a gradual increase in the CA oxidation peak current with an increase in CA concentration. The oxidation current of HQ is almost constant. This response proves that the oxidation of HQ and CA at SPCE\* occurs independently. The inset in Fig 8 shows dependence of SWV peak current on the concentration of HQ and CA. Clearly, HQ and CA oxidation peak current is increased linearly with the concentration, in the range of 0.5 to 50  $\mu\text{M}$  and 1.0 to 70  $\mu\text{M}$  for HQ and CA, respectively. However, the sensitivity (11.35  $\mu\text{A}/\mu\text{M}$  for HQ; 8.14  $\mu\text{A}/\mu\text{M}$  for CA) is smaller than those obtained in Fig. 7, which could be due to the current measurement difficulty regarding a very dilute concentration for one analyte in the presence of a relatively high concentration in another.

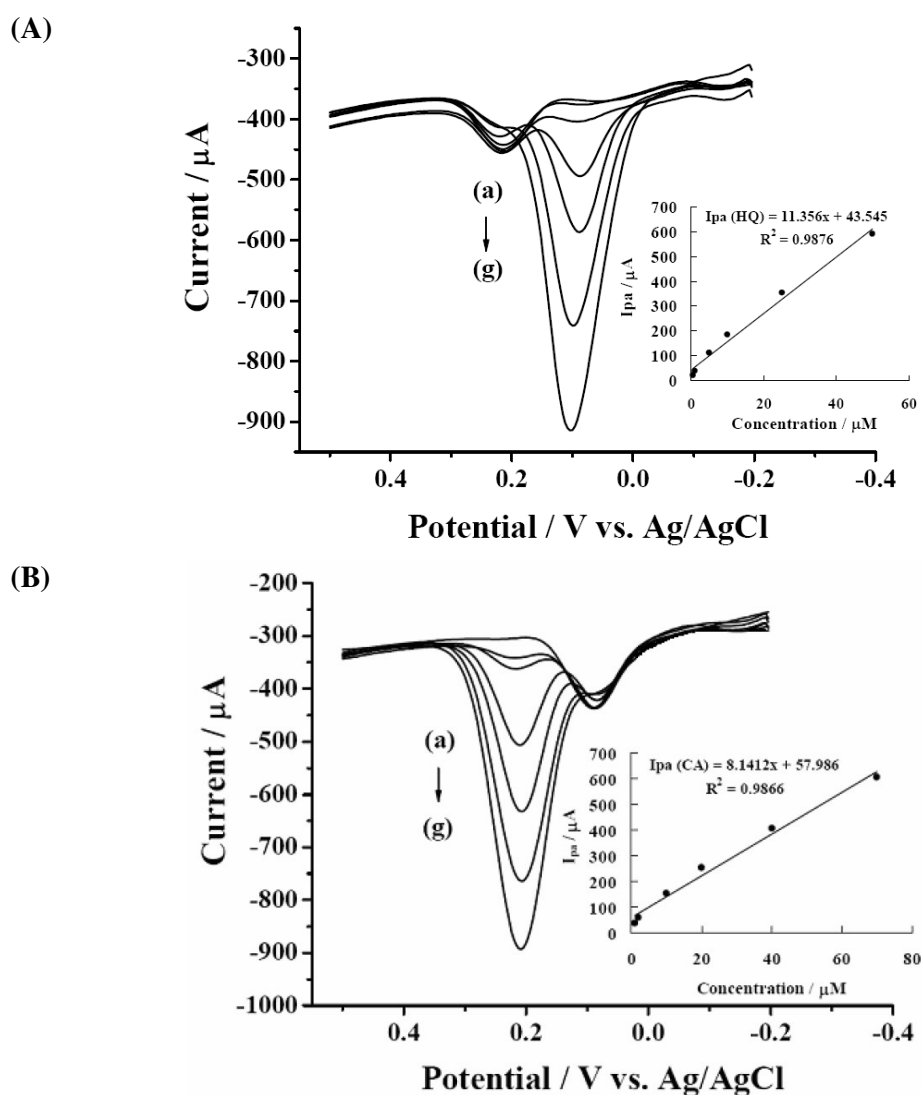


**Figure 8.** Square wave voltammograms at SPCE\* in pH 6.0 buffer solution containing (A) 0.5-50  $\mu\text{M}$  HQ in presence of 5  $\mu\text{M}$  CA (B) 1-70  $\mu\text{M}$  CA in presence of 5  $\mu\text{M}$  HQ. The inset shows the plot of  $I_{pa}$  vs. concentration.

The analytical performance of the proposed method is compared to previous reports based on the chemically modified electrodes, as shown in Table 1. Our method clearly offers the advantages of simple design, easy handling, high sensitivity, low detection limit and low cost. Table 2 shows the recovery tests for HQ and CA performed on a local river water sample. The collected river water was filtered, buffered to pH 6.0 and then spiked with varying concentrations of HQ and CA standard solution. The percentage recovery assays obtained recoveries of 98.6-108.4%, considered to be satisfactory recoveries. The results further substantiate that the proposed methods withstand analytical evaluation in monitoring of phenolic pollutants in river water.

#### 4. CONCLUSION

This study has demonstrated the feasibility of performing SWV to achieve a simultaneous determination of HQ and CA at SPCE\* in pH 6.0 buffer solution. The electrochemical preanodization is simple and SPCE\* shows effective adsorption of HQ and CA. The electrochemical pretreatment of electrode surfaces leads to morphological changes, large surface area, and more edge plane sites. These electrode features contribute to the molecular recognition, adsorption and high electroactivity.

Excellent analytical features were obtained that include: easy handling, good peak separation, high sensitivity, good linear dynamic range and a low detection limit. The proposed method was applied to an assay of HQ and CA in river water with good recoveries. This study provides a convenient route for the determination of dihydroxybenzene isomers and offers potentiality as a new analytical platform for various analytes in a mixture.

#### ACKNOWLEDGMENTS

The authors gratefully acknowledge the support provided by the National Science Council of the Republic of China under Grants NSC 98-2113-M-260-002-MY3.

#### References

1. Asan and I. Isildak, *J. Chromatogr. A*, 988 (2003) 145.
2. M.F. Pistonesi, M.S.D. Nezio, M.E. Centurion, M.E. Palomeque, A.G. Lista and B.S.F. Band, *Talanta*, 69 (2006) 1265.
3. P. Nagaraja, R.A. Vasantha and K.R. Sunitha, *J. Pharmaceut. Biomed.*, 25 (2001) 417.
4. J. Yuan, W. Guo and E. Wang, *Anal. Chem.*, 80 (2008) 1141.
5. N. Guan, Z.R. Zeng, Y.C. Wang, E.Q. Fu and J.K. Cheng, *Anal. Chim. Acta*, 418 (2000) 145.
6. R.M. de Carvalho, C. Mello and L.T. Kubota, *Anal. Chim. Acta*, 420 (2000) 109.
7. M. Del Pilar Taboada Sotomayor, A.A. Tanaka and L.T. Kubota, *Anal. Chim. Acta*, 455 (2002) 215.
8. I. Cruz Vieira and O. Fatibello-Filho, *Talanta*, 52 (2000) 681.
9. Y. Lei, G. Zhao, M. Liu, X. Xiao, Y. Tang and D. Li, *Electroanalysis*, 19 (2007) 1933.
10. M.A. Aziz, T. Selvaraju and H. Yang, *Electroanalysis*, 19 (2007) 1543.
11. Y.C. Tsai and C.C. Chiu, *Sens. Actuators B Chem.*, 125 (2007) 10.

12. G. A. M. Mersal, *Int. J. Electrochem. Sci.*, 4 (2009) 1167.
13. X.-G. Wang, Q.-S. Wu and Y.-P. Ding, *Electroanalysis*, 18 (2006) 517.
14. Y. Zhang and H. Zhuang, *Electrochim. Acta*, 54 (2009) 7364.
15. Z. Wang, H. Zhu, H. Zhang, G. Gao, Z. Sun, H. Liu and X. Zhao, *Electrochim. Acta*, 54 (2009) 7531.
16. Z.H. Wang, S.J. Li and Q.Z. Lv, *Sens. Actuators B Chem*, 127 (2007) 420.
17. P. Yang, W. Wei and L. Yang, *Microchim. Acta*, 157 (2007) 229.
18. Y.P. Ding, W.L. Liu, Q.S. Wu and X.G. Wang, *J. Electroanal. Chem.*, 575 (2005) 275.
19. M.A. Ghanem, *Electrochem. Commun.*, 9 (2007) 2501.
20. J. Yu, W. Du, F. Zhao and B. Zeng, *Electrochim. Acta*, 54 (2009) 984.
21. H. L. Qi and C.X. Zhang, *Electroanalysis*, 17 (2005) 832.
22. L. Wang, P. Huang, H. Wang, J. Bai, L. Zhang and Y. Zhao, *Int. J. Electrochem. Sci.*, 2 (2007) 216.
23. L. Wang, P. Huang, H. Wang, J. Bai, L. Zhang and Y. Zhao, *Int. J. Electrochem. Sci.*, 1 (2006) 403.
24. L. Wang, P. Huang, H. Wang, J. Bai, L. Zhang and Y. Zhao, *Int. J. Electrochem. Sci.*, 2 (2007) 123.
25. D. Zhang, Y. Peng, H. Qi, Q. Gao and C. Zhang, *Sens. Actuators B Chem*, 136 (2009) 113.
26. J.M. Zen, H.H. Chung, G. Ilangoan and A.S. Kumar, *Analyst*, 125 (2000) 1139.
27. C.C. Yang, A.S. Kumar and J.M. Zen, *Anal. Biochem.*, 338 (2005) 278.
28. F.Y. Song, F.S.C. Lee, and K.K. Shiu, *Electroanalysis*, 12 (2000) 128.
29. J.C. Chen, H.H. Chung, C.T. Hsu, D.M. Tsai, A.S. Kumar and J.M. Zen, *Sens. Actuators B Chem*, 110 (2005) 364.
30. J.C. Chen, A.S. Kumar, H.H. Chung, S.H. Chien, M.C. Kuo and J.M. Zen, *Sens. Actuators B Chem*, 115 (2006) 473.
31. X.P. Wu, L. Zhang, W.R. Liao, J.P. Duan, H.Q. Chen and G.N. Chen, *Electroanalysis*, 14 (2002) 1654.
32. K.S. Prasad, J.C. Chen, C. Ay and J.M. Zen, *Sens. Actuators B Chem*, 123 (2007) 715.
33. K.S. Prasad, G. Muthuraman and J.M. Zen, *Electrochem. Commun.*, 10 (2008) 559.
34. H.S. Wang, H.X. Ju and H.Y. Chen, *Electroanalysis*, 13 (2001) 1105.
35. T.H. Yang, C.L. Hung, J.H. Ke and J.M. Zen, *Electrochem. Commun.*, 10 (2008) 1094.
36. G. Cui, J.H. Yoo, J.S. Lee, J. Yoo, J.H. Uhm, G.S. Cha and H. Nam, *Analyst*, 126 (2001) 1399.
37. J. Wang, M. Pedrero, H. Sakslund, O. Hammerich and J. Pingarron, *Analyst*, 121 (1996) 345.
38. A.S. Kumar, S.S., P. Gayathri and J.M. Zen, *J. Electroanal. Chem.*, 641 (2010) 131.
39. A.S. Kumar and P. Swetha, *Langmuir*, 26 (2010) 6874.
40. C.E. Banks, T.J. Davies, G.G. Wildgoose and R.G. Compton, *Chem. Commun.*, (2005) 829.
41. R.T. Kachoosangi, C.E. Banks and R.G. Compton, *Electroanalysis*, 18 (2006) 741.
42. R.T. Kachoosangi and R.G. Compton, *Anal. Bioanal. Chem.*, 387 (2007) 2793.